



**HAL**  
open science

# Suitability of light scattering technique for measurements of water droplets in turbine wet steam flows

Simon Andres, Joachim Funcke, Manfred Wirsum, Thomas Polklas

► **To cite this version:**

Simon Andres, Joachim Funcke, Manfred Wirsum, Thomas Polklas. Suitability of light scattering technique for measurements of water droplets in turbine wet steam flows. 17th International Symposium on Transport Phenomena and Dynamics of Rotating Machinery (ISROMAC2017), Dec 2017, Maui, United States. hal-02390271

**HAL Id: hal-02390271**

**<https://hal.science/hal-02390271v1>**

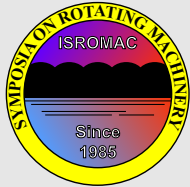
Submitted on 2 Dec 2019

**HAL** is a multi-disciplinary open access archive for the deposit and dissemination of scientific research documents, whether they are published or not. The documents may come from teaching and research institutions in France or abroad, or from public or private research centers.

L'archive ouverte pluridisciplinaire **HAL**, est destinée au dépôt et à la diffusion de documents scientifiques de niveau recherche, publiés ou non, émanant des établissements d'enseignement et de recherche français ou étrangers, des laboratoires publics ou privés.

# Suitability of light scattering technique for measurements of water droplets in turbine wet steam flows

Simon Andres<sup>1\*</sup>, Joachim Funcke<sup>1</sup>, Manfred Wirsum<sup>1</sup>, Thomas Polklas<sup>2</sup>



ISROMAC 2017

International  
Symposium on  
Transport Phenomena  
and  
Dynamics of Rotating  
Machinery

Maui, Hawaii

December 16-21, 2017

## Abstract

Suitability of light scattering technique for measurements of droplets in turbine wet steam flow depends on a variety of parameters. This paper examines all relevant aspects for droplet measurements inside low pressure steam turbines. On basis of light scattering theory, influence of these aspects for a distinct measurement of droplets is investigated. After clarification of these factors a discussion on measurement errors is given comprising errors that lie within the physics of light scattering theory as well as those caused by the measurement configuration. Possible avoidance by selection of proper measurement equipment and an elaborate design and setup of the probe is described including an estimation on each errors significance on measurement results. Light scattering technique is then evaluated on its applicability for low pressure steam turbines. It is argued in favor of light scattering that only measurements of single droplets provide insight into the fundamentals of droplet condensation and growth during expansion. Requirements for measurements with a light scattering probe in steam turbines regarding the system's design and composition are pointed out. Finally an outlook on present and future developments is given.

## Keywords

Mie theory, light scattering, wet steam, droplet measurements

<sup>1</sup> Institute for Power Plant Technology, Steam and Gas Turbines, RWTH Aachen University, Germany

<sup>2</sup> MAN Diesel & Turbo SE, Oberhausen, Germany

\*Corresponding author: andres@ikdg.rwth-aachen.de

## INTRODUCTION

The measurement of droplets in condensing flow in low pressure steam turbines has been a challenging task ever since. Optical techniques are capable of determining droplet sizes as well as overall wetness. However, by classification into primary and secondary droplets (fog and coarse droplets respectively) only certain of these technologies satisfy the required measuring needs. The distinction between primary and secondary droplets is made by means of their formation. Primary droplets are condensing spontaneously during expansion at the Wilson point. Secondary droplets break off from liquid films forming due to primary droplets wetting downstream blades. These coarse secondary droplets are responsible for blade erosion so that prevention of their generation or at least knowledge of their behaviour is desired (see for example [1]). In his extensive work on wet steam flows Gyarmathy [2] states that in every turbine stage approximately 1-5 % of primary droplets strike flow leading structures which potentially causes secondary droplets that have been breaking off blade trailing edges. He estimates that 5-30 % of wetness is provided by secondary droplets at the turbine exit. Contrary Williams and Lord [3] find the secondary droplet fraction to be maximally 8 % of total wetness where Cai et al. [4] measure values somewhere in between. However, for determination of the wetness fraction and the explicit thermodynamic state of the two-phase flow respectively, both primary and secondary droplets have to be measured. The importance for measurements of primary droplets is thereby increased by moving upstream from the

turbine exit whereas secondary droplets mostly appear and have to be measured towards the turbine outlet.

Kleitz and Dorey [5] as well as Moore and Sieverding [1] give a good overview on instrumentation of wet steam in general and also cover measurement of the immanent droplets. It is emphasized that optical measurement technologies have been proven superior to other approaches. Secondary droplets have been under investigation by means of several measurement techniques. The most recent developments have been made by Bosdas et al. [6] who use an optical backscatter probe with a shaft diameter of as small as 5 mm, Cai et al. [4] who designed an integrated probe for combined measurement of primary and secondary droplets using extinction and forward scattering that has a diameter of 20 mm and Bartos et al. [7], who also use a photogrammetric approach. Other optical probes have been introduced in earlier years. Kerckel et al. [8] developed a probe that utilizes two interfering beams to form the measuring volume; Fan et al. [9] designed a video-probe that takes pictures of very small exposure time to determine droplet sizes. Further approaches like shadowgraphy, holography and diffractometry can also be found and are described in Kleitz' and Dorey's work [5]. Opposite to the variety of measurement approaches for coarse droplets the measurement of primary droplets almost exclusively is done with light extinction probes. Early attempts by Walters [10], Tatsuno et al. [11] and Young et al. [12] provided a basis for all following probe designs. Recent studies on primary droplets have been performed by Schatz and Eberle [13] who use a wedge probe that is 10 mm in di-

ameter and that is also capable of measuring total and static pressures. Bosdas et al. [14] introduce a slightly smaller probe with heating to prevent contamination of the optical components and any other undesired beam disturbances.

Only Bohn et al. [15] - to the authors best knowledge - consider the light scattering technique for the measurement of primary droplets. The present work reinforces this judgement and points out principles, requirements, limitations and uniqueness of this technique.

## NOMENCLATURE

$d$	Droplet or particle diameter
$\underline{E}$	Electrical field
$\underline{H}$	Magnetic field
$I$	Electromagnetic wave intensity
$m$	Complex refractive index
$Q_{ext}$	Extinction efficiency
$r$	Radial distance
$\underline{S}$	Poynting vector
$We$	Weber number
$x$	Mie coefficient

## Symbols

$\theta$	Scattering angle
$\lambda$	Wavelength
$\rho$	Density
$\sigma$	Surface tension
$\phi$	Polarization angle

## Subscripts

0	Incident
$r$	Radial
$rel$	Relative
$s$	Scattered

## Abbreviations

CFD	Computational fluid dynamics
LP	Low pressure
MV	Measuring volume

## 1. LIGHT SCATTERING THEORY

At the very beginning shall be an introduction into the underlying physics. Discussion covers the intensity of light scattered by a spherical particle. Interested readers may be referred to Mie's [16] and Debye's [17] original work, as well as to Bohren and Huffmann [18], van de Hulst [19] or Jones [20] who, among others, give a good insight into scattering theory.

### 1.1 Fundamentals

The quantity of interest for the measurements is the intensity of the electromagnetic field scattered by a spherical particle which is specified by the absolute value of the Poynting vector

$$I = |\underline{S}| = |\underline{E} \times \overline{\underline{H}}| \quad (1)$$

with the electrical field  $\underline{E}$  and the magnetic field  $\underline{H}$  and its complex conjugate  $\overline{\underline{H}}$  respectively. For  $\underline{S}$  follows the vector product

$$\underline{S} = \underline{E} \times \overline{\underline{H}} = \begin{vmatrix} \underline{e}_1 & \underline{e}_2 & \underline{e}_3 \\ E_1 & E_2 & E_3 \\ \overline{H}_1 & \overline{H}_2 & \overline{H}_3 \end{vmatrix} \quad (2)$$

and for conversion into spherical coordinates

$$\underline{S} = - \begin{vmatrix} \underline{e}_r & \underline{e}_\phi & \underline{e}_\theta \\ E_r & E_\phi & E_\theta \\ \overline{H}_r & \overline{H}_\phi & \overline{H}_\theta \end{vmatrix}. \quad (3)$$

Note that only the scattered far field needs consideration in the discussed application so that it is assumed  $r \gg \lambda$ . Because the attenuation of the radial components is proportional to  $r^{-2}$  and of the tangential components only to  $r$ ,

$$E_r \wedge H_r \sim \frac{\lambda^2}{r^2}, E_\phi \wedge H_\phi \sim \frac{\lambda}{r}, E_\theta \wedge H_\theta \sim \frac{\lambda}{r}, \quad (4)$$

the vector product above simplifies to

$$\underline{S} = - \begin{vmatrix} \underline{e}_r & \underline{e}_\phi & \underline{e}_\theta \\ 0 & E_\phi & E_\theta \\ 0 & \overline{H}_\phi & \overline{H}_\theta \end{vmatrix} = (E_\theta \overline{H}_\phi - E_\phi \overline{H}_\theta) \underline{e}_r. \quad (5)$$

The energy of the diffracted wave therefore is only radiated into the  $\underline{e}_r$  direction as two intensity components perpendicular to each other

$$I_{\parallel} = I_0 \left( \frac{\lambda}{2\pi r} \right)^2 \cos^2 \phi S_2 \wedge I_{\perp} = I_0 \left( \frac{\lambda}{2\pi r} \right)^2 \sin^2 \phi S_1. \quad (6)$$

The amplitude functions

$$S_1 = \sum_{n=1}^{\infty} \frac{2n+1}{n(n+1)} (a_n \pi_n + b_n \tau_n) \quad (7)$$

and

$$S_2 = \sum_{n=1}^{\infty} \frac{2n+1}{n(n+1)} (a_n \tau_n + b_n \pi_n) \quad (8)$$

are composed of the scattering coefficients

$$a_n = \frac{m \psi_n(mx) \psi'_n(x) - \psi_n(x) \psi'_n(mx)}{m \psi_n(mx) \xi'_n(x) - \xi_n(x) \psi'_n(mx)} \quad (9)$$

and

$$b_n = \frac{\psi_n(mx) \psi'_n(x) - m \psi_n(x) \psi'_n(mx)}{\psi_n(mx) \xi'_n(x) - m \xi_n(x) \psi'_n(mx)} \quad (10)$$

and the angular functions

$$\pi_n = \frac{1}{\sin \theta} P_n^1(\cos \theta) \quad (11)$$

and

$$\tau_n = -\sin \theta \frac{P_n^1(\cos \theta)}{d(\cos \theta)}, \quad (12)$$

where  $\psi_n$  and  $\xi_n$  are a function of the spherical Bessel and Hankel functions of the first kind and  $P_n^1$  is the Legendre polynomial.

The scattering coefficients include the Mie-coefficient  $x$  which is given by the product of wavenumber and particle diameter

$$x = \frac{kd}{2} = \frac{\pi d}{\lambda} \quad (13)$$

and which is one of the most important parameters since its value allows conclusions about the type of scattering - for both small and large Mie coefficient values simplifications to the theory can be made.  $m$  denotes the ratio of complex refractive indices of particle and medium:

$$m = \frac{m_{\text{particle}}}{m_{\text{medium}}}. \quad (14)$$

The relative intensity of the scattered light is finally given as

$$\frac{I_s}{I_0} = \left( \frac{\lambda}{2\pi r} \right)^2 (\sin^2 \phi |S_1(\theta)|^2 + \cos^2 \phi |S_2(\theta)|^2). \quad (15)$$

It can be seen that the relative light scattering intensity depends on the incident light wavelength(s), the refractive indices of particle and surrounding media, the distance to the scatterer, the observation and the scattering angle, the light's polarization direction and of course the droplet size. Hereinafter the influence of these parameters on the relation between scattered light intensity and droplet size is discussed.

## 1.2 Theory utilization

The upper discussed theory can be implemented into computational tools with some little effort. A MATLAB tool developed by the author is capable of numerically calculating the relative scattered light intensity, accounting for all the aforementioned parameters according to the set and given boundary conditions such as the geometry of the probe, the light source and the exposed media.

However, simplifications are made by assuming unpolarized incident light and a constant refractive index. Unpolarized implies that the polarization of the light, which is in fact arbitrary in its orientation but distinct at every point in time and statistically evenly spread, changes too fast to be measured or - and this is the important assumption - to have an influence on the physical result of a measurement [21]. For unpolarized light, or to be more accurate, for the mean value of all occurring polarization states, integration over the whole polarization angle from 0 to  $2\pi$  gives the relative scattered light intensity

$$\frac{I_s}{I_0} = \frac{1}{2} \left( \frac{\lambda}{2\pi r} \right)^2 (|S_1(\theta)|^2 + |S_2(\theta)|^2) \quad (16)$$

since

$$\frac{1}{2\pi} \int_0^{2\pi} \cos^2 \phi \, d\phi = \frac{1}{2\pi} \int_0^{2\pi} \sin^2 \phi \, d\phi = \frac{1}{2}. \quad (17)$$

The refractive index was set to a real value of  $m = 1.33$ . Dependence of the refractive index subject to wavelength and fluid temperature has been modelled but neglected in the following calculations.

Due to the complexity of the underlying equations there is no possibility for optimization of the relevant parameters regarding the scattered light intensity to droplet diameter relation. The shown correlations therefore only show trends but cannot be considered as an optimum. An extensive parameter study would be needed to be confident of the optimum parameter values.

All given figures only show relative scattering intensities. It should be emphasized that a relative intensity value is sufficient for theoretical understanding since the measurements require a calibration anyway where absolute intensity values are assigned to known droplet sizes.

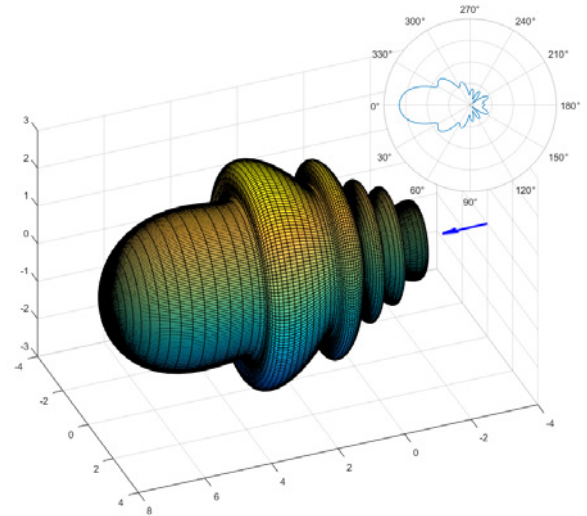


**Figure 1.** Logarithmic representation of the scattered light intensity around a spherical water droplet for a Mie coefficient of  $x = 7$

### 1.2.1 Scattered light intensity around a spherical water droplet

Fig. 1 shows the logarithmic relative scattered light intensity around a spherical water droplet of  $1 \mu\text{m}$  in diameter that is centred in the coordinate origin. It is lit by an electromagnetic wave with  $\lambda = 457 \text{ nm}$  which results in a Mie coefficient of approximately  $x = 7$ . In the top right corner the two-dimensional projection is given.

Most striking are the angular variance in scattering intensity amplitude and the non monotonous progression from

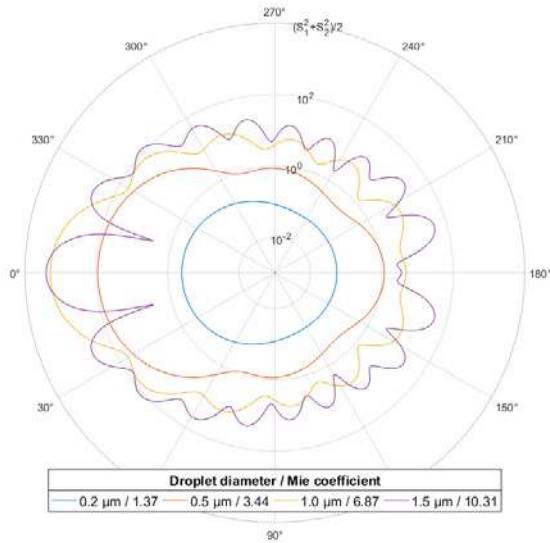


**Figure 2.** Logarithmic angular scattered light amplitude for particles with varying diameter and Mie coefficient respectively

backward to forward scattering. There would not be a difficulty in this if the proportion of the scattered light amplitudes for two particles would remain constant for all angles. But as can be seen in fig. 2 local minima and maxima of scattered light intensity change their angular position with varying particle diameter so that for a certain scattering angle there is no monotonous change in scattered light intensity and therefore no possibility of a distinct determination of particle size.

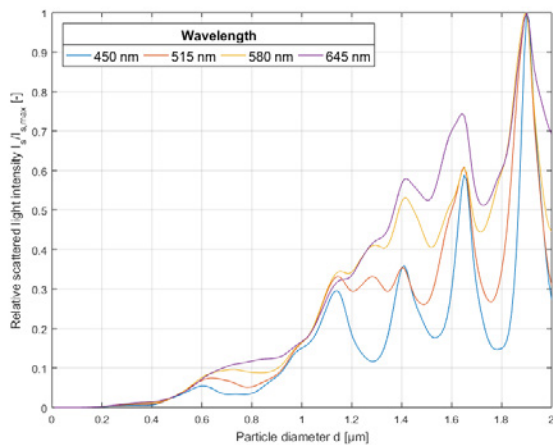


**Figure 3.** Relative scattered light intensity as a function of particle size for various wavelengths at a constant scattering angle of 90°

### 1.2.2 Dependence on wavelength

To counterbalance this circumstance the incident light might consist of multiple wavelengths. A change of wavelength for a certain particle size results in a change of the Mie coefficient, see eq. 13, and hence the relation between intensity and particle diameter differs. In fig. 3 the change of scattered light intensity with particle diameter is shown for different wavelengths at a constant scattering angle of 90°. The curve progressions seem to be arbitrary without any regularity, especially for droplets greater 1 μm in diameter. However it can be assumed that proper assembling of multiple wavelengths leads to smoothing of the curve progression. Since the water droplets of interest are in a size range from 0 to 2 μm plotting of scattered light intensity for larger droplets will be omitted - see sec. 3.

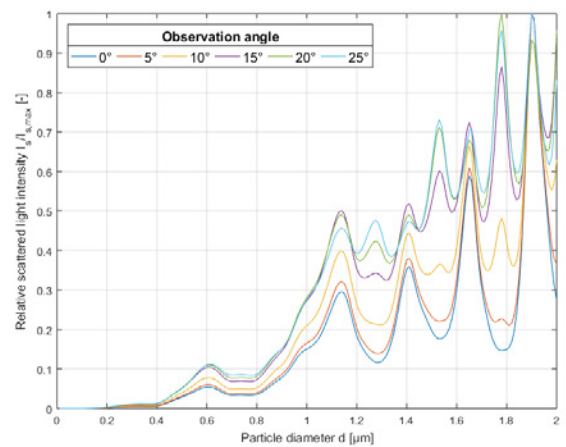


**Figure 4.** Relative scattered light intensity as a function of particle size for various observation angles at a constant scattering angle of 90° for a single wavelength

### 1.2.3 Dependence on observation angle

Further smoothing is also achievable and almost inevitable by introducing an observation angle. The reception of the scattered light requires an optical system that necessarily holds an observation angle - however small it might be. Enlarging this angle has two positive effects. First it increases the absolute received scattered light energy and second it flattens the irregularities in angular scattered light intensity as seen in fig. 2 by averaging the intensity over a specific angular range. Fig. 4 shows the variance of the scattered light intensity for rising observation angles; the particle is lit by monochromatic light. It is clearly visible that a large observation angle improves the explicitness of scattered light intensity concerning the particle diameter, especially for particle sizes above 1 μm. Use of multiple wavelengths further improves this relation.

### 1.2.4 Dependence on mean scattering angle

Another possibility of changing the correlation between scattered light intensity and particle diameter is given by changing the mean scattering angle. From fig. 5 it can be concluded



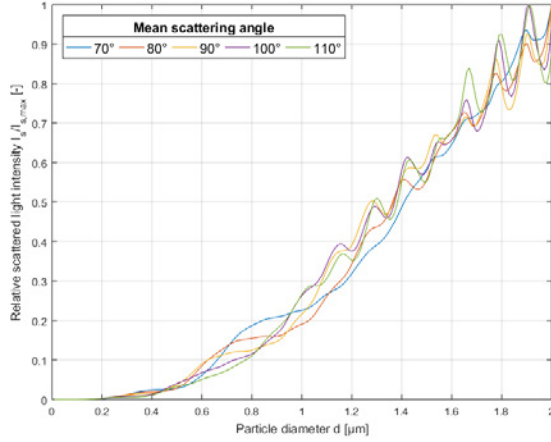


**Figure 5.** Relative scattered light intensity as a function of particle size for various mean scattering angles at a constant observation angle of  $25^\circ$

that small mean scattering angles are favourable for measurements. The choice of a fixed observation angle in combination with an average scattering angle will determine the curve progression of scattered light intensity regarding the particle diameter. As seen in fig. 2 small scattering angles relate to forward scattering where also the absolute scattered light intensity increases which benefits the signal strength and hence its processing.

As a **conclusion** of this section fig. 6 contrasts the scattered light intensity progression for a basic single wavelength and scattering angle calculation to an optimized calculation, where the above described enhancing factors have been applied. For the optimized configuration the relation of scattered light intensity and particle diameter is explicit and therefore the measurement technique is theoretically suitable for primary droplet measurements.

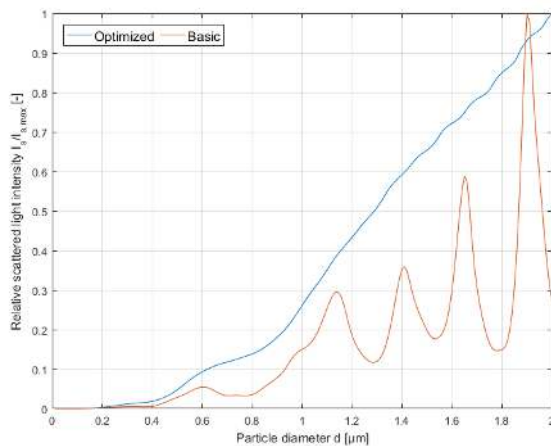


**Figure 6.** Relative scattered light intensity as a function of particle size for an optimized and a basic calculation

## 2. MEASUREMENT ERRORS

In this section a short treatise about measurement errors occurring during light scattering measurements shall be conducted. For each measurement error an estimation on its significance shows the influence on the measurement results.

### 2.1 Extinction

A laser beam that propagates straightly from the probe window to the measuring volume forms a cylinder. A laser beam that di- or converges from the probe window to the measuring volume forms a truncated cone. In these volumes enclosed droplets cause an attenuation of the laser beam, generally known as extinction. The scattered light emitted from the droplet in the direction of the receiver suffers from extinction as well. It should be self-evident that - for a constant droplet size distribution - the extinction rises the more droplets lie within the upper mentioned cylinders or truncated cones. The main influences on the magnitude of the extinction error are therefore the droplet density in the measuring environment and the size and shape of the laser beam imaging the measuring volume including the distance between the probe window and the measuring volume.

Total avoidance of the extinction error cannot be accomplished as long as droplets pass the beam that propagates towards the measuring volume and from the MV towards the receiver. Nevertheless, extinction can be minimized by proper selection of the optical path if the given particle density in the investigated flow is constant. In case of assurance that droplets only pass the measuring volume - for example through local seeding - extinction can be neglected.

Estimation of this error can be carried out in respect to assumed droplet size distributions. The effect of a monodispersed droplet size distribution is contrasted to a polydispersed size distribution. Firstly, the droplet density per volume needs to be considered. As seen in sec. 3 droplet densities in LP steam turbines are said to be  $10^6$  to  $10^7$  per  $\text{mm}^3$ .

The general relation for attenuation of a beam due to extinction is

$$\ln\left(\frac{I_0}{I_0 - I_{ext}}\right) = \frac{4\pi k z}{\lambda} \quad (18)$$

For multiple droplets of single size inside a medium the equation expands to

$$\ln\left(\frac{I_0}{I_0 - I_{ext}}\right) = N Q_{ext} \frac{\pi d^2}{4} z \quad (19)$$

and for multiple droplets that have a certain distribution in size to

$$\ln\left(\frac{I_0}{I_0 - I_{ext}}\right) = \sum_i N(d_i) Q_{ext} \frac{\pi d_i^2}{4} z. \quad (20)$$

$Q_{ext}$  denotes the so called extinction efficiency

$$Q_{ext} = \left(\frac{2\lambda}{d\pi}\right)^2 \text{Re}\{S(0^\circ)\} \quad (21)$$

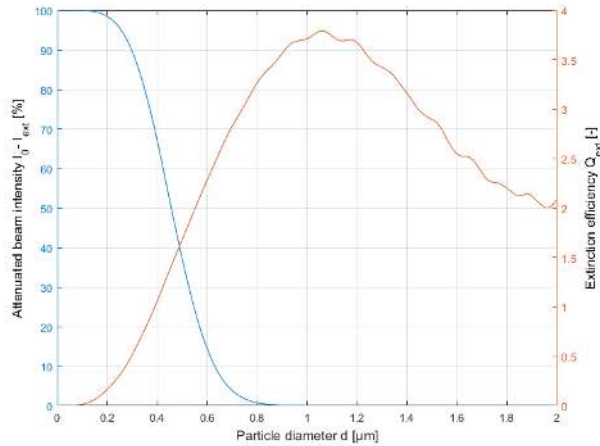


**Figure 7.** Extinction coefficient for polychromatic light and resulting beam intensity for different particle sizes assuming a monodispersed droplet size distribution

and is a function of particle diameter, wavelength and the specific value of the amplitude function for  $\theta = 0^\circ$ .

In fig. 7 the percentage of attenuation of a polychromatic light source is given for a constant droplet density for monodispersed droplets. It clearly shows that all droplets smaller than  $0.2 \mu\text{m}$  have almost no impact on the beam intensity whereas all droplets bigger  $0.8 \mu\text{m}$  lead to an almost full attenuation of the incident light. The edge steepness in between those values is correspondingly large. When assuming a droplet size distribution, for example as given by Petr and Kolovratnik [22], the attenuation of the beam is only about 0.5 %. As seen above this changes dramatically with the given size distribution and linearly with the droplet density and the illuminated path.

## 2.2 Beam expansion

The beam expansion error comes hand in hand with extinction since extinction equals the absorption of the particle medium plus its scattering.

In consequence, if we assume absorption in water to be neglectable – the imaginary part of the refractive index of water which denotes the absorption is in the range of  $10^{-9}$  to  $3.35 \times 10^{-8}$  for visible light [23] – all attenuation of the laser beam is due to scattering at the extinction causing droplets. It could therefore be a possibility that the amount of scattered light into the forward direction – towards the measuring volume – affects the intensity distribution in a non-neglectable manner so that the striven sharpness of the measuring volume is reduced. The significance of this error is assessable when falling back on the calculated extinction error. At worst all light that is lost due to extinction can make a change in intensity distribution. As for the upper calculated case with the droplet density distribution from Petr and Kolovratnik [22] this is about 0.5 % of the incident light. Hence the beam expansion error seems to be neglectable, at least for this case. Reconsideration may be important for

other circumstances.

## 2.3 Coincidence

To achieve reliable results it has to be ensured that only one droplet at a time is situated inside the measuring volume. The shape and the size of the measuring volume are a key to this. However there always is a certain possibility of two or more droplets being inside the measuring volume at the same time. The misinterpretation of multiple droplets as one is called coincidence. A special type of coincidence occurs when one particle leaves while another enters the measuring volume instantaneously. Depending on the measurement analysis system and setup it can also be a source of error which is called dynamic coincidence.

As Kleitz and Dorey [5] mention the coincidence as "one of the most serious limitations" of light scattering technique there shall be a closer look on how to deal with this error.

A way to reduce coincidence is by adapting the measuring volume size to the maximal droplet density. The catch is that the droplet density has to be known previous to the measurements and adaptations to the optical system of the probe are required. The measuring volume then can be generated as small as necessary that only a single droplet is lit simultaneously.

Detection of coincidence can be done at high measuring card sampling rates. The slope of the scattered pulse edge should not change while a droplet passes the measuring volume. In case there is a change of slope this could be an indicator for the entry of a second droplet into the measuring volume. These pulses should be excluded from the evaluation. Depending on their percentage share in regard to the overall measurement and assuming that those droplets follow the overall size distribution the droplet number can be corrected subsequently to obtain the actual quantity. Another practical way to identify coincidence requires a uniform intensity profile across the measuring volume and the beam axis. An elaborate design of the probe's optics can assure a reasonably even distribution. Droplets entering the MV at different times are distinguishable by means of the overall pulse height.

Dynamic coincidence - however small the possibility may be - can neither be exposed nor quantified.

## 2.4 Illumination error

This error is caused by a non-uniform intensity distribution inside the measuring volume, mostly one of Gaussian shape. In particular, a smaller droplet flying through the middle of the measuring volume produces the same scattering intensity as a bigger droplet flying through an outlying area. Statistical correction of this error can be applied for assuming a uniform droplet distribution over time and space. Since the same amount of droplets with the same sizes cross each part of the measuring volume correction factors can be applied to the pulse distribution that increase the amplitude of a certain share of all pulses just by the ratio of actual and maximum beam intensity. Physical correction by applying different optics resulting in a constant intensity distribution inside the MV is also a good possibility.

## 2.5 Side error

Besides multiple droplets staying inside the measuring volume at the same time it is also possible that a droplet only scratches the edge of the illuminated volume. In this case just a part of the scattered light is received by the sensor and the droplet will be underestimated in size. This is called side error. Besides the small pulses that are generated by side errored droplets these pulses are normally very short in time so that detection is rather difficult. This however helps avoiding side errors if for example a pulse width limit can be applied to the measurement values.

## 2.6 Multiple scattering

Another possible error arises from multiple scattering. If a droplet A lies within the measuring volume and is additionally illuminated by the scattered light of a droplet B (that for example lies behind the measuring volume but is also illuminated by the laser beam) the scattered light of droplet A will be a superposition from the scattered light with the laser's incident intensity and droplet B's scattered intensity. Since forward scattered light intensity is normally much bigger compared to intensities in all other angles - this effect diminishes for smaller droplets - the additional light scattering intensity introduced by droplet B will be negligible over the scattered light intensity originating from the laser beam. In addition, lit droplets inside the measuring volume scatter light in not only the direction of the sensor but everywhere. Droplets outside the measuring volume are subject to illumination by this scattered light and scatter light themselves into all directions – also towards the sensor. This share seems neglectable as well when compared to the main scattered light intensity originated from the laser beam. Jones [20] says that the distance between particles has to be three times their diameter to neglect multiple scattering.

## 3. APPLICATION TO DROPLET MEASUREMENTS IN LP STEAM TURBINES

Mie theory can only be applied if certain requirements are met. Droplets need to be spherical and homogeneous without surface charge as well as isolated and surrounded by a homogeneous and loss-free medium [16]. The incident light has to be a planar harmonic wave of infinite extent with known intensity - which also implies that phase and amplitude of the wave should be constant across the particle. For particle clouds Jones [20] additionally expresses that the particles need random arrangement yielding incoherent scattering, have no interaction of their electromagnetic fields among each other and are only lit by unscattered light - that multiple scattering is neglectable, respectively. The satisfaction of these requirements will be part of this section.

Droplets of special interest in this paper are the so called primary droplets that nucleate because of expansion of the steam. Due to its surface tension a droplet levitating in space will always try to attain a spherical shape [1]. It is due to other on the droplet acting forces that it will deform and eventually

break up into smaller droplets. The ratio of these forces and the droplet surface tension, expressed by the Weber number

$$We = \frac{\rho_g w_{rel}^2 d}{\sigma}, \quad (22)$$

is an indicator for deformation and break up of droplets. Since the relative velocity  $w_{rel}$  between gaseous and liquid phase for droplets forming within the flow during condensation can be assumed to be zero there is no droplet deformation. Slip between droplets and steam caused by flow deflection is negligible for droplets smaller  $1 \mu\text{m}$  [1]. On the other hand secondary droplets e.g. from blade trailing edges are much bigger, have a high difference in velocity compared to the steam and are therefore very sensitive to deformation and break up. A good overview on breakup modes depending on Weber numbers is given by Kékesi et al. [24].

Homogeneity of the primary droplets is given material and temperature wise due to their small size. In water dissolved salts and other foreign objects could induce inhomogeneity but since the power plant feed water is usually completely demineralized this is disregarded.

Bohren and Huffman [18] give some information on charged spherical particles. A quantitative evaluation is not made but it is assumed that surface charge only has a slight impact on scattering and absorption properties.

The droplets' surrounding medium - steam - is isolated from the droplets due to its gaseous state and assumed homogeneous since any inhomogeneities would lead to further scattering at these impurities. Steam is considered loss-free - meaning it has negligible absorption - as are the water droplets.

Illumination of the particle depends on the optical system and whether the beams is collimated or converging. A collimated beam can be seen as a planar wave since its focal point lies at infinity. A convergent beam can rather be approximated as a spherical wave. Weyl [25] however shows that a spherical wave can be expressed as a superposition of many plane waves of miscellaneous direction.

Of the three requirements expressed by Jones [20] for particle clusters the first and third need no consideration since the formation of droplets and hence also their arrangement are arbitrary and multiple scattering has already been treated during error estimation in sec. 2.6. Interaction of the droplets' electromagnetic fields is dependent on their quantity per volume. Jones therefore gives maximum particle concentrations that are  $10^{19}$  per  $\text{m}^3$  for  $0.1 \mu\text{m}$  particles,  $10^{16}$  per  $\text{m}^3$  for  $1.0 \mu\text{m}$  particles and so forth. Droplet densities in wet steam turbines have been found to be  $10^{15}$  to  $10^{16}$  per  $\text{m}^3$  [22][26]. Gyarmathy [2] and Seibold [27] predict primary droplet sizes of up to  $0.6 \mu\text{m}$ . In other literature also sizes of up to  $4 \mu\text{m}$  are reported but directly neglected due to their marginal occurrence. Most authors believe primary droplets ranging in sizes from  $0.1$  to  $1 \mu\text{m}$ . From this point of view interaction among the droplets in LP wet steam flow should have no importance for Mie theory application.



#### 4. DESIGN OF A MEASUREMENT SYSTEM

A probe for measurements of primary droplets inside LP steam turbines needs to meet certain conditions. As Bosdas et al. [6] point out access holes in steam turbines usually are in a diameter range of 8 to 15 mm. The probe's diameter should therefore also lie in this range to ensure maximum accessibility. Other conditions also arise from the above cited sections.

The light source should be strong in power to compensate for the relatively small scattered light intensity and polychromatic to improve the correlation of scattered light intensity and droplet diameter. A multi-line laser therefore seems appropriate. Insertion of the laser beam into the probe should be done through optical fibers. In order to allow for decoherization of the incident polychromatic light by smoothing the speckle contrast a multimode fiber of an appropriate length can be used for transportation of the laser beam into the probe head [28]. Another advantage of a laser is its focusability. Theoretically for monochromatic light a focal point with almost no extent is feasible. Even though the use of polychromatic light should be of choice it can generate an adequate spot size if some effort is put into the design of the imaging system.

To cope with coincidence the measuring volume should be as small as possible and the beam intensity inside the measuring volume should be of different than a Gaussian shape, preferably uniform. Based on a droplet concentration of  $10^{15} - 10^{16}$  droplets per  $m^3$  the minimum edge length of the measuring volume, implying a cubic volume, calculates to  $4.6 - 10 \mu m$ . However, regarding the droplet size distribution calculated by Petr and Kolovratnik [22] that state droplet sizes from as small as  $0.01 \mu m$  a lower resolution limit has to be set in order to distinguish measured droplet pulses from measurement noise. Assumption of a lower resolution limit of  $0.1 \mu m$  leads to exclusion of about 70 % of droplets which however are due to their small size only responsible for 15 % of the wetness fraction. The permissible edge length then rises to  $6.9 - 14.9 \mu m$ . Hence it gives an advantage to set a higher minimum resolution limit allowing the enlargement of the measuring volume without coincidence of two or more droplets. On the other hand the measurement error rises because of the increased minimum resolution limit just by the wetness fraction of the excluded droplets. For a uniformly lit MV it can be enlarged and coincident droplets can be detected by the superposition of their scattered light intensities assuming that they are not entering the measurement volume at the same time. To prevent droplet deposition on the optical components of the probe a purging air flow on these surfaces should be realized.

Accornero and Maretto [29] found axial Mach numbers between 0.6 and 0.85 at the exit of a 320 MW steam turbine which imply velocities of up to  $300 m/s$ . For measurement of primary droplets that follow the steam flow without slip a high sampling measured value acquisition is needed. For the upper case a droplet passes a measurement volume of  $10 \mu m$  in diameter in 33 ns. Hence a system with a sampling rate of

approximately 1 GHz should be used.

Due to the primary droplets' small size only a few measurement techniques are feasible for their determination. Most approaches include the light extinction method that admittedly has its disadvantages. Only light scattering technique is able to measure single droplets and hence gives an exact droplet size distribution. Extinction suffers from matching distribution functions to the actual measurement results and can therefore only estimate the real size distribution. An accurate understanding of the nucleation of droplets in wet steam flow can therefore only be achieved by application of the light scattering technique.

#### 5. CONCLUSION AND OUTLOOK

This paper theoretically proves the suitability of light scattering techniques for droplet size measurements in low pressure steam turbines. Through the treatment of the underlying physical theory it is shown that the choice of the incident light source as well as the geometrical setup of the probe and the position of the measuring volume respectively have a major impact on the technique's applicability. Furthermore conditions in the low pressure turbine as a measurement environment determine the setup and design of the probe and the measurement system.

On one hand, due to the measurement of single droplets, this technique helps further understanding of the phenomenology of nucleating wet steam flows. On the other hand it helps to reduce the still existing mismatch between calculated condensing flows in CFD simulations by providing the opportunity for adjustment of the underlying models.

Further development of the already mentioned probe by Bohn et al. [15] is currently promoted at RWTH Aachen University with an aim of miniaturization and application to a 12 MW model steam turbine.

#### ACKNOWLEDGEMENTS

The investigations were conducted as part of the joint research program COOREFLEX-turbo in AG Turbo. The work was supported by the Bundesministerium für Wirtschaft und Technologie (BMWi) under file number 03ET7071S on the basis of a resolution of the German Parliament. The authors gratefully acknowledge AG Turbo and MAN Diesel & Turbo SE for their support and permission to publish this paper. The responsibility for the content of this publication lies with the authors.

#### REFERENCES

- [1] M. J. Moore and C. H. Sieverding. *Two-phase steam flow in turbines and separators: Theory, instrumentation, engineering*. Series in thermal and fluids engineering. Hemisphere Pub. Corp, Washington, 1979.
- [2] Georg Gyarmathy. *Grundlagen einer Theorie der Nassdampfturbine*. Dissertation, ETH, Zürich, 1962.

- [3] G. J. Williams and M. J. Lord. Measurement of coarse water distribution in the l.p. cylinders of operating steam turbines. *ARCHIVE: Proceedings of the Institution of Mechanical Engineers 1847-1982 (vols 1-196)*, 190(1976):59–69, 1976.
- [4] X. Cai, D. Ning, J. Yu, J. Li, L. Ma, C. Tian, and W. Gao. Coarse water in low-pressure steam turbines. *Proceedings of the Institution of Mechanical Engineers, Part A: Journal of Power and Energy*, 228(2):153–167, 2014.
- [5] A. Kleitz and J. M. Dorey. Instrumentation for wet steam. *Proceedings of the Institution of Mechanical Engineers, Part C: Journal of Mechanical Engineering Science*, 218(8):811–842, 2004.
- [6] Ilias Bosdas, Michel Mansour, Anestis I. Kalfas, and Reza S. Abhari. An optical backscatter probe for time resolved droplet measurements in turbomachines. *Measurement Science and Technology*, 27(1):015204, 2015.
- [7] Ondrej Bartos, Xiaoshu Cai, and Michal Kolovratnik. A detection of the coarse water droplets in steam turbines. *EPJ Web of Conferences*, 67:02005, 2014.
- [8] S. W. Kerchel, M. L. Simpson, M. Azar, and M. Young. An optical technique for characterizing the liquid phase of steam at the exhaust of an lp turbine. *Office of Scientific and Technical Information (OSTI)*, 24, 1993.
- [9] Xueliang Fan, Zhihai Jia, Jingjing Zhang, and Xiaoshu Cai. A video probe measurement system for coarse water droplets in lp steam turbine. *Journal of Physics: Conference Series*, 147:012065, 2009.
- [10] P. T. Walters. Wetness and efficiency measurements in l.p. turbines with an optical probe as an aid to improving performance. *Journal of Engineering for Gas Turbines and Power*, 109(1):85, 1987.
- [11] K. Tatsuno and S. Nagao. Water droplet size measurements in an experimental steam turbine using an optical fiber droplet sizer. *Journal of Heat Transfer*, 108(4):939, 1986.
- [12] J. B. Young, K. K. Yau, and P. T. Walters. Fog droplet deposition and coarse water formation in low-pressure steam turbines: A combined experimental and theoretical analysis. *Journal of Turbomachinery*, 110(2):163, 1988.
- [13] M. Schatz and T. Eberle. Experimental study of steam wetness in a model steam turbine rig: Presentation of results and comparison with computational fluid dynamics data. *Proceedings of the Institution of Mechanical Engineers, Part A: Journal of Power and Energy*, 228(2):129–142, 2014.
- [14] Ilias Bosdas, Anestis I. Kalfas, Michel Mansour, and Reza S. Abhari. A miniature optical extinction heated probe for fog droplet measurements in steam turbines. *Biannual Symposium on Measuring Techniques in Turbomachinery*, XXIII, 2016.
- [15] D. Bohn, J. Funcke, J. Ren, N. Suerken, M. Sell, and T. Osterhage. Numerical and experimental investigation of the wetness in the front stages of a low-pressure steam turbine. *VGB PowerTech*, 11, 2004.
- [16] Gustav Mie. Beiträge zur optik trüber medien, speziell kolloidaler metallösungen. *Annalen der Physik*, 330(3):377–445, 1908.
- [17] P. Debye. Der lichtdruck auf kugeln von beliebigem material. *Annalen der Physik*, 335(11):57–136, 1909.
- [18] Craig F. Bohren and Donald R. Huffman. *Absorption and Scattering of Light by Small Particles*. Wiley-VCH Verlag GmbH, Weinheim, Germany, 1998.
- [19] H. C. van de Hulst. *Light scattering by small particles*. Dover and London : Constable, New York, 1981.
- [20] A. R. Jones. Light scattering for particle characterization. *Progress in Energy and Combustion Science*, 25(1):1–53, 1999.
- [21] Henry Hurwitz. The statistical properties of unpolarized light. *Journal of the Optical Society of America (1917-1983)*, 35(8):525, 1945.
- [22] V. Petr and M. Kolovratnik. Modelling of the droplet size distribution in a low-pressure steam turbine. *Proceedings of the Institution of Mechanical Engineers, Part A: Journal of Power and Energy*, 214(2):145–152, 2000.
- [23] George M. Hale and Marvin R. Query. Optical constants of water in the 200-nm to 200- $\mu$ m wavelength region. *Applied Optics*, 12(3):555–563, 1973.
- [24] T. Kékesi, G. Amberg, and L. Prahl Wittberg. Drop deformation and breakup. *International Journal of Multiphase Flow*, 66:1–10, 2014.
- [25] H. Weyl. Ausbreitung elektromagnetischer wellen über einem ebenen leiter. *Annalen der Physik*, 365(21):481–500, 1919.
- [26] D. E. Bohn, N. Sürken, and F. Kreitmeier. Nucleation phenomena in a multi-stage low pressure steam turbine. *Proceedings of the Institution of Mechanical Engineers, Part A: Journal of Power and Energy*, 217(4):453–460, 2003.
- [27] Andreas Seibold. *Entwicklung einer hoch auflösenden Sonde zur simultanen Erfassung von Kondensations- und Strömungsvorgängen in Niederdruck-Dampfturbinen: Zugl.: Stuttgart, Univ., Diss., 2004*, volume 524 of *Fortschritt-Berichte VDI Reihe 6, Energietechnik*. VDI-Verl., Düsseldorf, als ms. gedr edition, 2004.
- [28] H. Nakano, N. Miyanaga, K. Yagi, K. Tsubakimoto, T. Kanabe, M. Nakatsuka, and S. Nakai. Partially coherent light generated by using single and multimode optical fibers in a high-power nd: Glass laser system. *Applied Physics Letters*, 63(5):580–582, 1993.
- [29] M. J. Moore and C. H. Sieverding. *Aerothermodynamics of low pressure steam turbines and condensers*. Hemisphere, Washington, 1987.